

Another view to Pismis 3 with 2MASS Photometry

Tadross, A. L. *

National Research Institute of Astronomy and Geophysics, 11421 - Helwan,
Cairo, Egypt

Abstract This paper is a continuation of a series, aiming to refine and re-determine the most physical parameters of rarely or/and un-studied open star clusters with a good quality CMDs using Near-IR *JHK* photometry. A morphological analysis of (*2MASS*) database (the digital "Two Micron All Sky Survey") has been presented for the open cluster Pismis 3. The only previous work for this cluster has been introduced by Carraro & Ortolani (1994). In the present work, some physical properties estimated for the first time and some others re-determined whereas they can be compared with the previous study.

Key words: techniques: photometric — Galaxy: open clusters and associations stars: luminosity function, mass function: individual: Pismis 3

1 INTRODUCTION

A deep photometric and astrometric analysis in the open star cluster Pismis 3 has been presented here using *2MASS*¹ database. The *2MASS* Surveys has proven to be a powerful tool in the analysis of the structure and stellar content of open clusters (cf. Bonatto & Bica 2003, Bica et al. 2003). It is uniformly scanning the entire sky in three near-IR bands *J*(1.25 μm), *H*(1.65 μm) and *K_s*(2.17 μm) with two highly automated 1.3-m telescopes equipped with a three channel camera, each channel consisting of a 256 \times 256 array of HgCdTe detectors. The photometric uncertainty of the data is less than 0.155 mag with *K_s* \sim 16.5 mag photometric completeness. Further details can be found at the web site of *2MASS*.

Pismis 3 (C0829-3830, OCL 731) is situated in the southern Milky Way at 2000.0 coordinates $\alpha = 08^{\text{h}} 31^{\text{m}} 22^{\text{s}}$, $\delta = -38^{\circ} 39' 00''$; $\ell = 257.865^{\circ}$, $b = +0.502^{\circ}$. Carraro & Ortolani (1994), hereafter CO94, obtained *CCD BV* photometry for Pismis 3 and its nearby field. Their analysis suggests that it is of intermediate age (about 2 Gyr) and metal poor ($Z = 0.008$) cluster. They derived a color excess $E(B-V) = 1.35$, and an apparent distance modulus (m-M) = 14.70 mag (about 1.5 Kpc distant from the Sun). In our series, the most fundamental parameters have been estimated, i.e. age, reddening, distances (from the sun; the galactic

* E-mail: altadross@nriag.sci.eg

¹ <http://www.ipac.caltech.edu/2MASS>

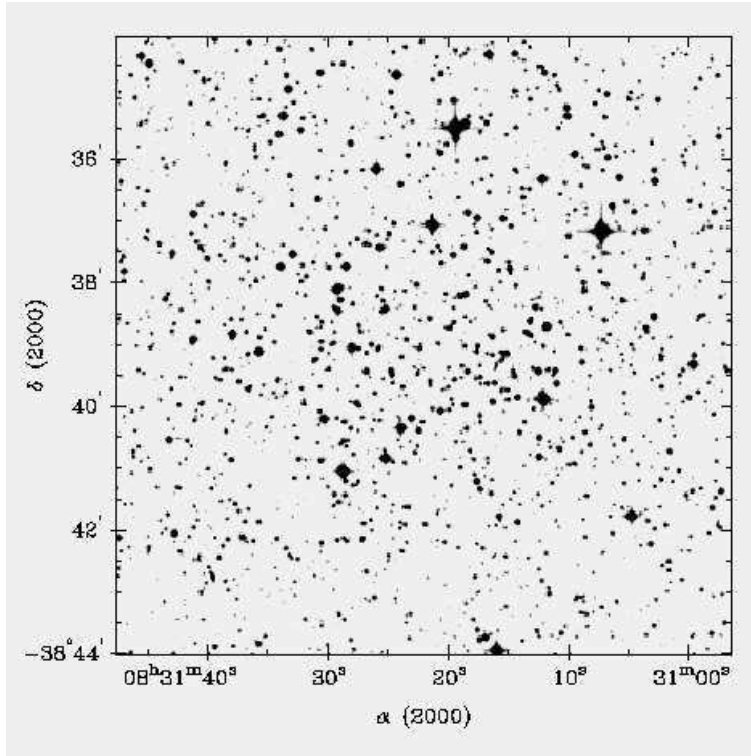


Fig. 1 The blue image of Pismis 3 as taken from Digitized Sky Surveys (*DSS*). North is up, east on the left.

plane; the galactic center), diameters (cluster's border; core radius; tidal radius), luminosity function, mass function, total mass, relaxation time, and mass segregation. Relevant examples are NGC 1883; NGC 2059; NGC 7086 (Tadross 2005), and NGC 7296 (Tadross 2006). This paper is organized as follows: Sect. 2, data extraction; Sect. 3, cluster center & radii; Sect. 4, *CMD* analysis (membership richness - reddening - distances - age, and metallicity); Sect. 5, luminosity function; Sect. 6, mass functions & total mass; Sect. 7, mass segregation & dynamical state; and finally the conclusions have been summarized and listed with a comparing table in Sect. 8. Fig. 1 represents the blue image of Pismis 3 as taken from Digitized Sky Surveys (*DSS*)². It takes the name from the astronomer who in the late fifties (Pismis 1959) who compiled a catalogue of 2 globular and 24 new open star clusters in the Galactic Plane between $\ell = 225^\circ$ and $\ell = 353^\circ$ (cf. CO94).

2 DATA EXTRACTION

Data extraction have been performed using the known tool of VizieR³. The number of stars in the direction of Pismis 3 within a preliminary radius of 10 arcmin is found to be 4390 stars. In order to maximize the statistical significance

² <http://cadwww.dao.nrc.ca/cadcbn/getdss>

³ <http://vizier.u-strasbg.fr/viz-bin/VizieR?-source=2MASS>

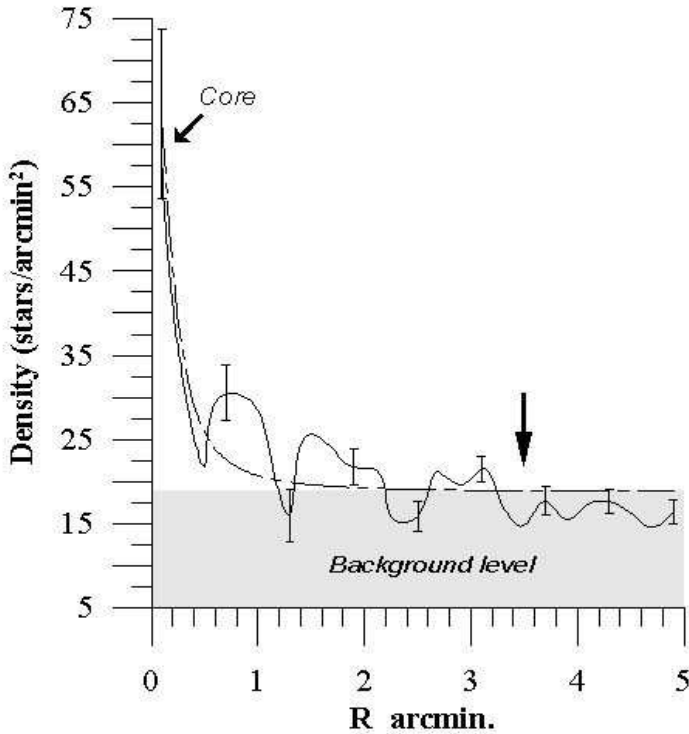


Fig. 2 Radial distribution of the surface density of Pismis 3 (solid curve). The vertical short bars represent the Poisson errors. The dashed line represents the fitting of King (1962). The upper arrow refers to the core region, and the lower one marks the apparent minimum radius of the cluster. The dark region represent the mean level of the offset field density, which taken at ~ 18 stars per arcmin^2 .

and representativeness of background star counts, an external area (the same area as the cluster) has been used as offset field sample. This external sample lies at 1 degree away from the cluster's center.

Before counting stars for estimating the cluster's properties with *JHK 2MASS* photometry, we applied a cutoff of photometric completeness ($J < 16.5$) to both cluster and offset field to avoid over-sampling, i.e. to avoid spatial variations in the number of faint stars which are numerous, affected by large errors, and may include spurious detections (Bonatto et al. 2004). Also, in this respect, for more accuracy, we restricted to stars with observational uncertainties $\epsilon_{J, H, K} < 0.2$ mag.

3 THE CLUSTER CENTER AND RADII

The cluster center is define as the location of maximum stellar density of the cluster's area. The cluster center is found by fitting a Gaussian to the profiles of star counts in right ascension (α) and declination (δ), see Tadross 2004, 2005 and 2006. The estimated center is found to lie at $\alpha = 127.84089 \pm 0.003$ and

$\delta = -38.64478 \pm 0.002$ degrees, which is found to differ from WEBDA⁴ by 0.2 sec in right ascension and 18.8 arcsec in declination.

To determine the cluster's minimum radius, core radius and tidal radius, the radial surface density of the stars $\rho(r)$ should be achieved firstly. The tidal radius determination is made possible by the spatial coverage and uniformity of 2MASS photometry, which allows one to obtain reliable data on the projected distribution of stars for large extensions around clusters (Bonatto et al. 2005). In this context, the background contribution level corresponds to the average number of stars included in the offset field sample is found to be ~ 18 stars per arcmin². Applying the empirical profile of King (1962), the cluster's minimum apparent radius is taken to be 3.5 arcmin, as shown in Fig. 2. Knowing the cluster distance from the sun in parsecs (§ 4), the cluster and core radii are found to be 2.2 and 0.2 pc respectively. Applying the equation of Jeffries et al. (2001), the tidal radius (R_t) of Pismis 3 is found to be ~ 12 pc. Consequently, the distances of the cluster from the galactic plane, Z , and its projected distances from the Sun, X_\odot , Y_\odot , are found to be 18.0 pc; -2.0 , and 0.44 kpc respectively. The distance from the galactic center, R_g , is found to be 8.7, or 8.0 kpc using the galactocentric distance of the sun $R_o = 8.0$, or 7.2 kpc according to Reid (1993), or Bica et al. (2006) respectively. It is found that R_g is consenting with; but Z is larger than what obtained by Salaris et al. (2004).

4 COLOR-MAGNITUDE DIAGRAM ANALYSIS

Because of the low galactic latitude of Pismis 3, the background field of the cluster is found to be crowded (≈ 18 stars per arcmin²), and the observed *CMD* is contaminated. Fig. 3 represents the *CMD* of Pismis 3, showing the magnitude completeness limit and the color filter for the stars within the apparent cluster radius, whereas 450 stars are classified as cluster members. The membership criteria here is adopted for the location of the stars in the *CMD*, which must be close to the cluster main sequence (the stars lie between the two dashed curves in Fig. 3, which have "+" signs), the maximum departure accepted here is about 0.15 mag. On this base, the fundamental photometrical parameters of the cluster (reddening, distance modulus, age, and metal content) can be determined simultaneously, by fitting one of Padova isochrones to the *CMD* of the cluster.

In this respect, several fittings have been applied on the $J \sim (J - H)$ of Pismis 3 using Bonatto et al. (2004) isochrone of solar metallicity with different ages. $R_V = 3.2$, $A_J = 0.276 \times A_V$, and $E(J - H) = 0.33 \times E(B - V)$ have been used for reddening and absorption transformations, according to Dutra, Santiago & Bica (2002) and references therein. The overall shape of the *CMD* is found to be well reproduced with isochrones of 2.24 Gyr in age. The apparent distance modulus is found to be 12.20 ± 0.10 mag, accordingly the intrinsic one, $(m - M)_o$, is found to be 11.60 ± 0.10 mag, corresponding to a distance of 2090 ± 95 pc. On the other hand, the color excess, $E(J - H)$, is found to be 0.22 mag, which turns out to be $E(B - V) = 0.67$ mag. It is found that $[\text{Fe}/\text{H}]$ is consenting with; but the age is smaller than what obtained by Salaris et al. (2004). It is worthily to mention that the noticed differences of the main parameters for Pismis 3 between the present work and CO94 is mainly due to the difference of the metal content of the used isochrone.

⁴ <http://obswww.unige.ch/webda/navigation.html>

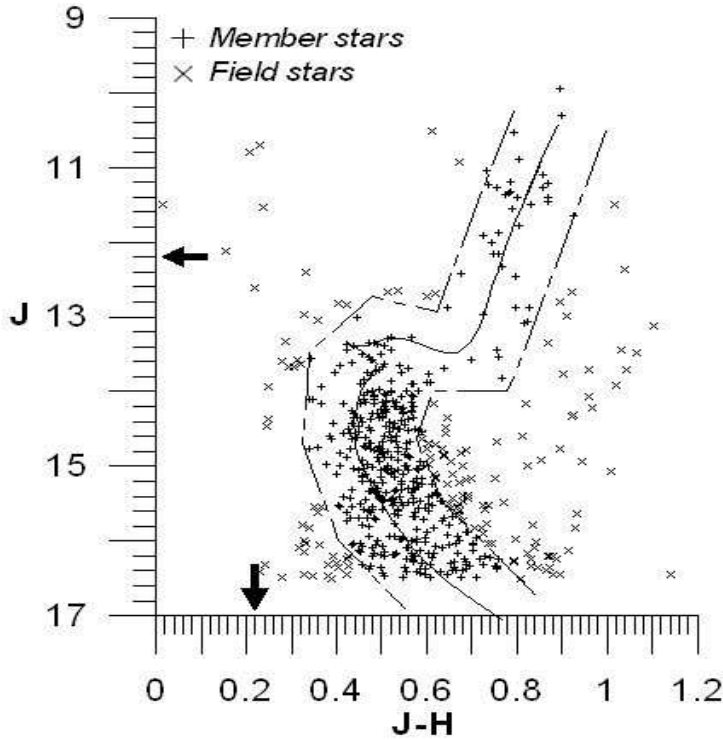


Fig. 3 Padova solar isochrone with $\log \text{age} = 9.35$ (2.24 Gyr) is fitted to the $J \sim (J - H)$ CMD of Pismis 3. Dashed curves represent the color and magnitude filters used in reducing the field contamination of the cluster. The horizontal and vertical arrows refer to the values of distance modulus and color excess on the vertical and horizontal axes respectively.

5 LUMINOSITY FUNCTION

The observed stars have been counted in terms of the absolute magnitude M_J after applying the distance modulus derived above. The color and magnitude filters cutoffs have been applied to the cluster and offset field stars. The magnitude bin interval are taken to be $\Delta M_J = 0.50$ mag. In Fig. 4, the LF constructed as the difference in the number of stars in a given magnitude bin between the cluster's stars (dashed area) and the offset field ones (white area). Dotted area represents the background subtracted LF . The scale of observed J magnitude appears along the upper axis of Fig. 4. From the LF of Pismis 3, we can infer that more massive stars are more centrally concentrated whereas the beak value lies at fainter magnitude bin (Montgomery et al. 1993). This peak corresponds to $J \approx 15.3$ mag, i.e. $M_J \approx 3.7$ mag.

6 MASS FUNCTION AND TOTAL MASS

Given the luminosity function, the mass function and then the total mass of the cluster can be derived. To derive the MF from LF , the theoretical evolutionary

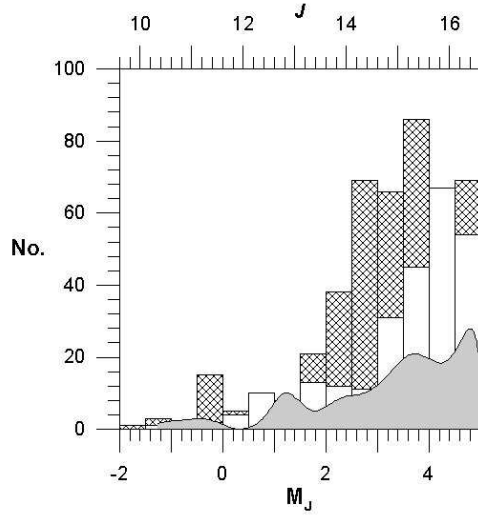


Fig. 4 Spatial distribution of luminosity function for Pismis 3 in terms of the absolute magnitude M_J . The color and magnitude filters cutoffs have been applied to the cluster (dashed area) and the offset field (white area). The dark curved area represents the background subtracted LF . The scale of observed J magnitude appears along the upper axis.

track of Bonatto et al. (2004) with solar metal abundance ($Z=0.019$) and age of 2.24 Gyr is used. In this sense, a polynomial equation of fourth degrees has been used for the cluster members in the range of $-1.75 \leq M_J \leq 4.75$ as following:

$$\mathcal{M}/\mathcal{M}_{\odot} = 3.13 - 0.66 M_J - 0.10 M_J^2 + 0.051 M_J^3 - 0.005 M_J^4$$

Step-plot has been constructed for the cluster stellar masses showing the number of stars at 0.5 intervals between $0.65 \sim 3.65 \mathcal{M}_{\odot}$, as shown in Fig. 5. Using a least-square fit, the slope of IMF is found to be $\Gamma = -2.37 \pm 0.25$, which is about in agreement with the value of Salpeter (1955). In this respect, the total mass of the cluster has been estimated by summing up the stars in each bin weighted by the mean mass of that bin. It yields a minimum cluster mass of $\sim 560 \mathcal{M}_{\odot}$.

It is noted that, unresolved binaries and low mass stars are problems for this technique. In this respect, Van Albada & Blaauw (1967) assumed that 60% of early type stars are double systems, whereas Jaschek & Gomez (1970) claimed that approximately 50% of the main sequence stars might be hidden (cf. Bernard & Sanders 1977). According these assumptions, the total mass of the cluster Pismis 3 can be reached to $\sim 800 \mathcal{M}_{\odot}$.

7 MASS SEGREGATION AND DYNAMICAL STATE

For a dynamically relaxed cluster, the higher mass stars are expected to be settled toward the cluster center, while the fainter, lower mass stars are residing in the outer regions of the cluster, Mathieu (1984). The existence of mass segregation is due to the dynamical evolution or/and imprint of star formation process. At the time of formation, the cluster may have a uniform spatial stellar mass distribution, and because of the dynamical relaxation, low mass stars may possess the largest random velocities, trying to occupy a larger volume than the

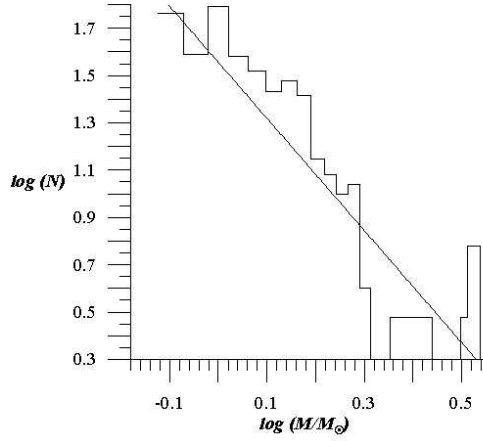


Fig. 5 The mass function of Pismis 3. The slope of the initial mass function *IMF* is found to be $\Gamma = -2.37 \pm 0.25$; with correlation coefficient of 0.90.

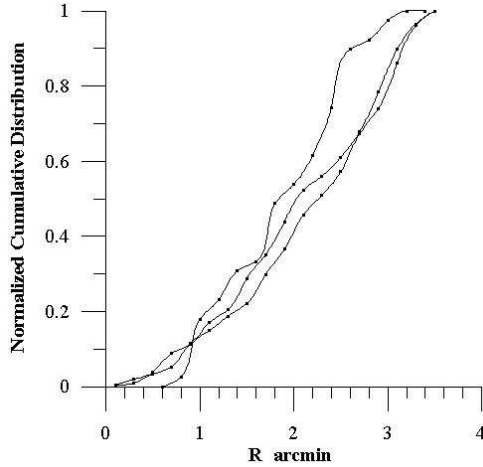


Fig. 6 Mass segregation in Pismis 3. Moving from left to right, the curves represent the mass ranges $\mathcal{M}/\mathcal{M}_{\odot} > 2.0$; ($M_J : -0.1 \sim 1.5$), $1.0 \leq \mathcal{M}/\mathcal{M}_{\odot} \leq 2.0$; ($M_J : 1.6 \sim 3.6$), and $\mathcal{M}/\mathcal{M}_{\odot} < 1.0$; ($M_J : 3.6 \sim 4.9$). This indicates that the bright massive stars accumulate much more quickly with radius than the fainter low mass stars do.

high mass stars do (cf. Mathieu & Latham 1986, McNamara & Sekiguchi 1986, Mathieu 1985).

To display mass segregation in Pismis 3, star counts are performed on the main sequence as a function of distances from the cluster center and masses. The results are given in Fig. 6. The individual curves moving from left to right are for mass ranges $\mathcal{M}/\mathcal{M}_{\odot} > 2.0$, $1.0 \leq \mathcal{M}/\mathcal{M}_{\odot} \leq 2.0$, and $\mathcal{M}/\mathcal{M}_{\odot} < 1.0$. It

suggests that the brighter high mass stars concentrate towards the cluster center and accumulate much more quickly than the fainter low mass stars do. On the other hand, we are interested if the cluster reached the dynamical relaxation or not. Applying the dynamical relaxation' equation (cf. Tadross 2005 & 2006), it is found to be 8.6 Myr, which implies that the cluster age is ~ 260 times its relaxation one. Thus we can conclude that Pismis 3 is dynamically relaxed and the evolution is one of the possible cause of mass segregation.

8 CONCLUSIONS

According our analysis for refining and determining the fundamental parameters of Pismis 3 using *2MASS* photometry, the present results are summarized and compared with the previous one (CO94) in table 1.

Acknowledgements This publication made use of the Two Micron All Sky Survey (*2MASS*), which is a joint project of the University of Massachusetts and the Infrared Processing and Analysis Center California Institute of Technology, funded by the National Aeronautics and Space Administration and the National Science Foundation. Catalogues from *CDS/SIMBAD* (Strasbourg), and Digitized Sky Survey *DSS* images from the Space Telescope Science Institute have been employed.

References

- Bernard, J., Sanders, W.L., 1977, *A&A*, 54, 569
 Bica, E., Bonatto, Ch., Dutra, C.M., 2003, *A&A*, 405, 991
 Bica, E., Bonatto, Ch., Barbuy, B., Ortolani, S., 2006, *A&A*, 450, 105
 Bonatto, Ch., Bica, E., 2003, *A&A*, 405, 525
 Bonatto, Ch., Bica, E., Girardi, L., 2004, *A&A*, 415, 571
 Bonatto, Ch., Bica, E., Santos, J.F., 2005, *A&A*, 433, 917
 Carraro, G., Ortolani, S., 1994, *A&A*, 291, 106
 Dutra, C., Santiago, B., Bica, E., 2002, *A&A*, 381, 219
 Jaschek, C., Gomez, A.E., 1970, *PASP*, 82, 809
 Jeffries, R.D., Thurston, M.R., Hambly, N.C., 2001, *A&A*, 375, 863
 King, I., 1962, *AJ*, 67, 471
 Lyngå, G., 1987, Catalog of Open Cluster Data, Centre des Donée astronomiques de Strasbourg
 Mathieu, R., 1984, *ApJ*, 284, 643
 Mathieu, R., 1985, Dynamics of star clusters 113, 427 (J. Goodman and P. Hut eds.)
 Mathieu, R., Latham, D., 1986, *AJ*, 92, 1364
 McNamara, B., Sekiguchi, K., 1986, *ApJ*, 310, 613
 Montgomery, K.A., Marschall, L.A., Janes, K.A., 1993, *AJ*, 106, 181
 Pismis, P., 1959, *Bol. Obs. Tonantzintla Tacubaya* 18, 39
 Reid, M.J., 1993, *ARA&A*, 31, 345
 Salaris, M., Weiss, A., Percival, S., 2004, *A&A*, 414, 163
 Salpeter, E., 1955, *ApJ*121, 161
 Spitzer, L., Hart, M., 1971, *ApJ*, 164, 399
 Tadross, A.L., 2004, *Chin. J. Astron. Astrophys. (ChJAA)*, 4, 67
 Tadross, A.L., 2005, *AN* 326 (1), 19
 Tadross, A.L., 2006, *AN* 327 (7), 714

Table 1 Comparisons between the present study and CO94

Parameter	The present work	CO94
Center	$\alpha = 08^h 31^m 21.8^s$ $\delta = -38^\circ 38' 41.2''$	$08^h 29^m 6^s$ $-38^\circ 30' 0''$
Age	2.24 Gyr.	2.0 Gyr.
Metal abundance	0.019	0.008
$E(B - V)$	0.67 mag.	1.35 mag.
R_v	3.2	3.0
Distance Modulus	12.20 ± 0.10 mag.	14.70 mag.
Distance	2090 ± 95 pc.	1500 pc.
Radius	$3.5'$ (2.20 pc.)	$3.25'$
Membership	450 stars	--
$E(J - H)$	0.22 mag.	--
ρ_o	63 ± 2 stars/arcmin ²	--
Core radius	$0.19' \pm 0.04$ (0.20 pc)	--
Tidal radius	12 pc.	--
R_g	$8.7 \sim 8.0$ kpc. (see § 3)	--
Z	18 pc.	--
X_\odot	-2.0 kpc.	--
Y_\odot	0.44 kpc.	--
Luminosity fun.	Estimated	--
IMF slope	$\Gamma = -2.37 \pm 0.25$	--
Total mass	$\approx 560 \mathcal{M}_\odot$ (minimum)	--
Relaxation time	8.6 Myr	--
Mass segregation	Achieved	--

Trumpler, R.J., 1930, LOB 14, 154

Van Albada, T., Blaauw, A., 1967, CoORB, Uccle B17, 44